Inorganic Chemistry

Article

pubs.acs.org/IC

Excellent Selectivity for Actinides with a Tetradentate 2,9-Diamide-1,10-Phenanthroline Ligand in Highly Acidic Solution: A Hard−Soft Donor Combined Strategy

Cheng-Liang Xiao,[†] Cong-Zhi Wang,[†] Li-Yong Yuan,[†] Bin Li,[‡] Hui He,[‡] Shuao Wang,[§] Yu-Liang Zhao,[†] Zhi-Fang Chai,*[,†,§] and Wei-Qun Shi*[,†]

[†]Key Laboratory of Nuclear Radiation and Nuclear Energy Technology and Key Laboratory For Biomedical Effects of Nanomaterials and Nanosafety, Institute of High Energy Physics, Chinese Academy of Sciences, Beijing 100049, P.R. China

[‡]Division of Radiochemistry, China Institute of Atomic Energy, Beijing 102413, P.R. China

[§]School of Radiological and Interdisciplinary Sciences, Soochow University, Suzhou 215123, P.R. China

Supporting Information

ABSTRACT: In this work, we reported a phenanthroline-based tetradentate ligand with hard−soft donors combined in the same molecule, *N*,*N*′-diethyl-*N*,*N*′-ditolyl-2,9-diamide-1,10-phenanthroline (Et-Tol-DAPhen), for the group separation of actinides over lanthanides. The synthesis and solvent extraction as well as complexation behaviors of the ligand with actinides and lanthanides are studied experimentally and theoretically. The ligand exhibits excellent extraction ability and high selectivity toward hexavalent, tetravalent, and trivalent actinides over lanthanides in highly acidic solution. The chemical stoichiometry of Th(IV) and U(VI) complexes with Et-Tol-DAPhen is determined to be 1:1 using X-ray crystallography. The stability constants of some typical actinide and lanthanide complexes of Et-Tol-DAPhen are also determined in methanol by UV−vis spectrometry. Density functional theory (DFT) calculations reveal that the An−N bonds of the Et-Tol-DAPhen complexes have more covalent characters than the corresponding Eu−N bonds, which may in turn lead to the selectivity of Et-Tol-DAPhen toward actinides. This ligand possesses merits of both alkylamide and 2,9-bis-(5,6-dialkyl-1,2,4-triazin-3-yl)-1,10-phenanthroline (R-BTPhen) extractants for efficient actinide extraction and the selectivity toward minor actinides over lanthanides and hence renders huge potential opportunities in high-level liquid waste (HLLW) partitioning.

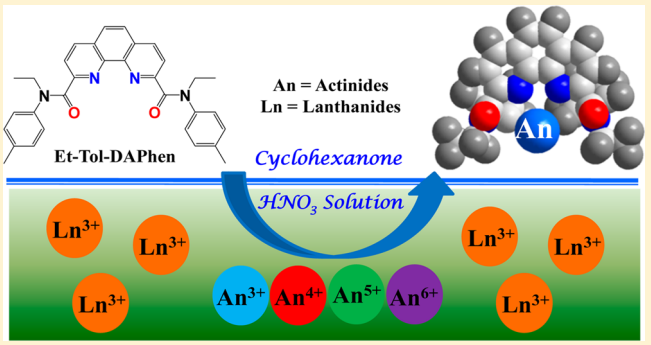

INTRODUCTION

After the emergence of nuclear power plants, the environmental issues associated with spent fuels accompanying electricity generation have been of great concern.[1] Though U and Pu can be recovered by the traditional PUREX (Plutonium and Uranium Recovery by Extraction) process, minor actinides (MA) still remaining in the high-level liquid waste (HLLW) become the predominant long-lived radiotoxic elements and will pose long-term risks toward the environment. The so-called partitioning and transmutation (P and T) strategy[2−4] may provide a reasonable approach to achieve the minimization of nuclear waste and to reduce the threat of MA.

To avoid nuclear proliferation and meet the requirements of the nuclear fuel cycle in the Generation IV nuclear energy system, a conceptual GANEX (Group ActiNide EXtraction) process[5−10] was proposed to recover almost all actinides (U, Np, Pu, Am, and *Cm*) together from highly acidic spent fuel solution. After the first cycle for the selective separation of uranium with a monoamide extractant, transuranium elements in varous oxidation states are simultaneously extracted using a multiple extractant system in the second cycle. Actually, several extractant-combined systems have been investigated preliminarily, such as tributyl phosphate (TBP) and 2,6-bis(5,6-dialkyl-1,2,4-triazin-3-yl)-2,2′-bipyridine (R-BTBP)[5,8−10]/2,9-bis-(5,6-dialkyl-1,2,4-triazin-3-yl)-1,10-phenanthroline (R-BTPhen)[5] (Figure 1), *N*,*N*-di-2-ethylhexyl-butylamide (DEHBA) and R-BTBP (Figure 1),[7] *N*,*N*,*N*′,*N*′-tetra-*n*-octyl-diglycolamide (TODGA), and *N*,*N*′-dimethyl-*N*,*N*′-dioctyl-2-(2-hexyloxyethyl)malonamide (DMDOHEMA).[6]

To simplify the GANEX process and improve the separation efficiency, a simple alternative extractant seems more promising in comparison with the multiple extractant combination. This is a difficult task because the challenge of the GANEX process comes from the separation of MA(III) from Ln(III). MA(III) and Ln(III) have similar chemical properties, such as oxidation state, ionic radius, hydration, and complexation mode. Extractants containing soft sulfur or nitrogen atoms are

Received: November 18, 2013

   dx.doi.org/10.1021/ic402784c | Inorg. Chem. XXXX, XXX, XXX−XXX

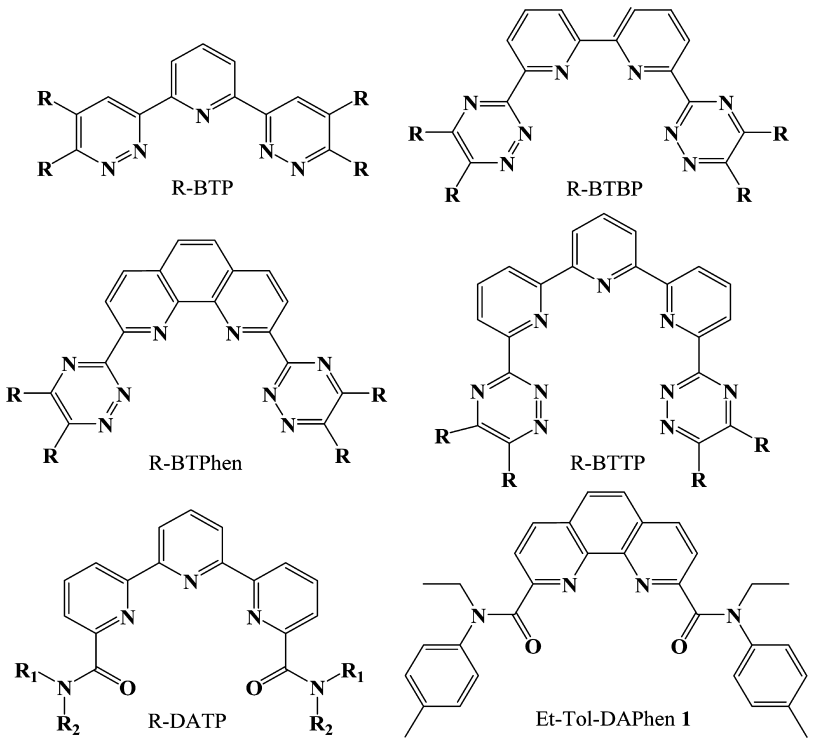

Figure 1. Promising ligands for lanthanide/actinide separation mentioned in this work.

Scheme 1. Synthesized Route of Ligand 1

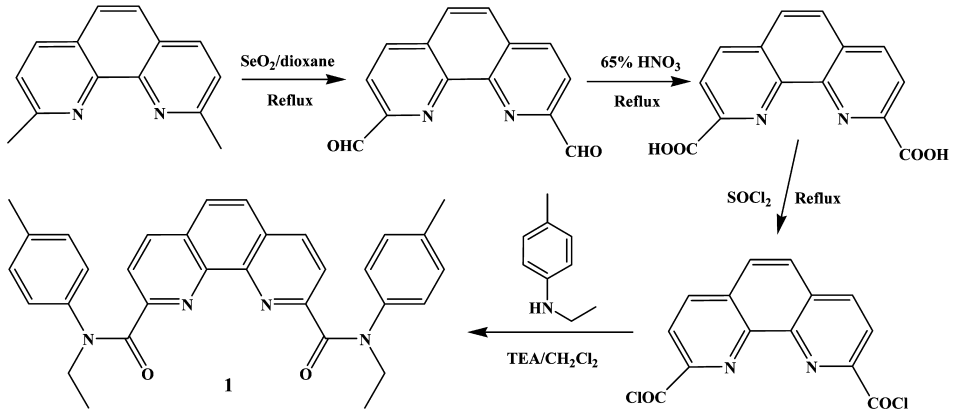

preferred to recognize MA(III) over Ln(III).[11−18] 2,6-Bis(5,6-dialkyl-1,2,4-triazin-3-yl)pyridine (R-BTP),[19−23] R-BTBP,[11,24−30] and R-BTPhen[16,24,27,31] ligands have been the successful representatives for the separation of Ln(III)/MA(III) in the past 15 years. However, light actinides (U, Np, Pu) normally favor ligands containing hard oxygen atoms such as alkylamide and alkylphosphate.[32−37] If solely considering the selectivity for light actinides using hard-donor ligands, the separation of MA(III) from Ln(III) would be difficult to achieve. Although some attempts to design single extractants for group separation of actinides from lanthanides have been carried out by Miguirditchian and his co-workers,[38,39] the distribution ratios of actinides and separation factors of actinides toward lanthanides are relatively low in highly acidic solutions. It is possible that the cavity of 6,6″-(2,2′:6′,2″-terpyridine)diamide (R-DATP)[38,39] (Figure 1) defined by the terpyridine and two amide groups does not match all actinides. In addition, the rotation of σ bonds linked with two pyridine heterocycles also hinders the complexation of the ligand with actinide ions. Additionally, Charbonnel et al.[40] reported a kind of 2,9-dipyridyl-l,10-phenanthroline ligands grafted with one or two amide groups, which showed difficult to separate all the actinides over lanthanides. Therefore, it is still highly desirable to design and synthesize more highly efficient extractants for selectively complexing all actinides over lanthanides.

In this work, we first synthesized and characterized a novel *N*-heterocyclic tetradentate ligand (ligand **1**) consisting of a phenanthroline moiety with soft nitrogen atoms showing selectivity for MA(III) over Ln(III) and two amide moieties with hard oxygen atoms in favor of light actinides, such as Th, U, Np, and Pu. The solvent extraction experiments of ligand **1** toward some actinides and lanthanides were investigated in cyclohexanone solvent. The crystal structures of ligand **1** with UO_2^{2+} and Th^{4+} were characterized to elucidate the extraction mechanism. The stability constants (log β) for some actinides and lanthanides complexes with ligand **1** were also determined

dx.doi.org/10.1021/ic402784c | *Inorg. Chem.* XXXX, XXX, XXX−XXX

in methanol by UV−vis spectrometry. To further understand the mechanism of exceptional selectivity for actinides, the coordination modes and bonding nature of ligand **1** with some actinide and lanthanide ions were studied by quantum chemical calculations with denstity functional theory (DFT) method.

EXPERIMENTAL SECTION

General. Chemical reagents such as rare earth nitrates $Ln(NO_3)_3 \cdot 6H_2O$ (Ln = La, Eu, and Yb), $UO_2(NO_3)_2 \cdot 6H_2O$, $Th(NO_3)_4 \cdot 5H_2O$, and other nitrate salts were of analytical grade. Stock solution of ^{241}Am in 1.0 M HNO_3 was provided by China Institute of Atomic Energy (CIAE). 2,9-Dimethyl-1,10-phenanthroline, selenium oxide, 1,4-dioxane, thionyl chloride, *N*-ethyl-*p*-toluidine, methanol, dichloromethane, and other inorganic/organic reagents were of analytical grade and used without further purification.

Nuclear magnetic resonance (NMR) spectra were measured on a Bruker Avance III 500 MHz spectrometer with tetramethylsilane as an internal solvent resonances reference. Fourier transform infrared spectroscopy (FT-IR) spectra were recorded on a Nicolet Nexus 670 Model instrument using the KBr self-supported pellet technique. Electrospray ionization mass spectrometry (ESI-MS) data was obtained on a Bruker Amazon SL instrument in the form of positive model.

Syntheses. The novel ligand **1** was synthesized according to Scheme 1. The syntheses of 2,9-dicarbaldehyde-1,10-phenanthroline and 2,9-dicarboxylic acid-1,10-phenanthroline were mildly modified on the basis of known procedures.[41,42]

2,9-Dicarbaldehyde-1,10-phenanthroline. Selenium oxide (5.62 g, 0.05 mol) was added into a mixture of 1,4-dioxane (150 mL) and deionized water (10 mL) in a 500 mL of three-necked flask. After heating to reflux, a solution of 2,9-dimethyl-1,10-phenanthroline (5.02 g, 0.024 mol) in 1,4-dioxane (100 mL) was added dropwise into the flask over 10 min. The reaction remained under reflux for 2 h. The mixture was filtered while hot, and the filtrate was left to cool. Yellow needle product (4.78 g, 82.36%) was obtained after filtering and washing with warm 1,4-dioxane. The crude product was used in the next step without further purification.

2,9-Dicarboxylic Acid-1,10-phenanthroline. 2,9-Dicarbaldehyde-1,10-phenanthroline (5.04 g, 0.021 mol) was added into a concentrated HNO_3 solution (65 wt %, 100 mL). After reaction under reflux for 3 h, the mixture was poured onto solid ice (∼20 g) and allowed to cool. The light-yellow solid (4.68 g, 83.15%) was crystallized and filtered from the mother liquor. The crude product was used in the next step without further purification.

N,N′-Diethyl-N,N′-ditolyl-2,9-diamide-1,10-phenanthroline. 2,9-Dicarboxylic acid-1,10-phenanthroline (2.02 g, 7.54 mmol) was refluxed with thionyl chloride (50 mL) in an inert atmosphere. After 3 h, the mixture was cooled, and thionyl chloride was removed by reduced pressure distillation. When the solvent was completely evaporated, the gray solid was dissolved in dichloromethane (50 mL) and cooled in ice water. Subsequently, *N*-ethyl-*p*-toluidine (4.03 g, 29.80 mmol) and triethylamine (6.04 g, 59.68 mmol) were added slowly into the mixture. The reaction was continued for 3 h at 40 °C under N_2 protection. The solvent was removed under reduced pressure. The residue was purified with silica gel column chromatography (eluent: $CH_3OH/CHCl_3$ = 1/50) and recrystallized from CH_3OH/CH_2Cl_2 to yield white powders of ligand **1** (1.82 g, 48.08%). ^1H NMR (500 Hz, $CDCl_3$) δ 1.35 (s, 6H, Ben-CH_3), δ 2.28 (t, 6H, CH_2CH_3), δ 4.11 (d, 4H, CH_2CH_3), δ 7.15 (s, 4H, Ben-*H*), δ 6.92 (s, 4H, Ben-*H*), δ 7.59 (d, 4H, Phen-*H*), δ 8.03 (s, 2H, Phen-*H*). FT-IR (KBr, ν/cm^{-1}): 1641 (amide), 1550, 1512, 1452, 1395, 1315, 1254, 1186, 1124, 866, 826, 721, 555. ESI-MS: m/z $(M + H)^+$ 503.2, $(M + Na)^+$ 525.3, $(M + K)^+$ 541.2. The ligand **1** crystals suitable for X-ray crystallographic measurement were obtained after slow evaporation from its methanol solution over several days.

$UO_2(NO_3)_2$ Complex Crystals ***2***. The ligand **1** (25.10 mg, 0.05 mmol) was dissolved in acetone (2 mL). To this mixture was added a solution of $UO_2(NO_3)_2 \cdot 6H_2O$ (25.12 mg, 0.05 mmol) in deionized water (2 mL). After stirring for half an hour, the solution was left to evaporate slowly. Flaky yellow crystals suitable for X-ray crystallographic measurement were obtained over 3 days.

$Th(NO_3)_4$ Complex Crystals ***3***. The ligand **1** (50.01 mg, 0.10 mmol) was dissolved in acetone (4 mL). To this mixture was added a solution of $Th(NO_3)_4 \cdot 5H_2O$ (57.02 mg, 0.10 mmol) in deionized water (4 mL). After stirring for half an hour, the solution was left to evaporate slowly. Light-yellow flaky crystals suitable for X-ray crystallographic measurement were obtained over 4 days.

Solvent Extraction Experiments. All the radioactive experiments were performed in the glovebox. The aqueous phases were prepared with stock solution of $^{241}Am^{3+}$, UO_2^{2+}, Th^{4+}, La^{3+}, Eu^{3+}, Yb^{3+}, Co^{2+}, Ni^{2+}, Zn^{2+}, and Sr^{2+} in different HNO_3 concentration (0.1−4.0 mol/L). The organic phases were prepared by dissolving ligand **1** (0.01 mol/L) in cyclohexanone. Each aqueous phase (1 mL) was vigorously shaken with each organic phase (1 mL) for 60 min at 25 °C. This contact time was enough to reach extraction equilibrium. After phase separation by centrifugation, the activity of α-ray emitters ^{241}Am was measured by a low-background α scintillation detector (FJ414, Beijing Nuclear Instrument Factory). The concentrations of other metal ions were determined by inductively coupled plasma optical emission spectrometry (ICP-OES, ULTIMA 2, Horiba). The distribution ratio (D) was calculated by the ratio between the concentration (radioactivity counts) in the organic phase and aqueous phase. The separation factor (SF) was calculated by the ratio of distribution ratios between two metal ions.

X-ray Crystallographic Measurements. X-ray crystallographic data were collected with graphite monochromated Mo−Kα radiation (λ = 0.71073 Å) at 293 K on a Bruker Apex II CCD diffractometer. Data treatments were carried out with the SAINT program.[43] The structures were solved using direct methods and refined on F_2 by full-matrix least-squares with the SHELXTL-97 program.[44] The non-hydrogen atoms were refined with anisotropic displacement parameters. The hydrogen atoms were placed by geometrical considerations and were added to the structure factor calculation. X-ray crystallographic data of ligand **1**, UO_2^{2+} complex **2**, and Th^{4+} complex **3** are summarized in Table S1, Supporting Information [SI]. Selected bond distances and angles are listed in Tables S2−S4, SI.

UV−Vis Spectrophotometric Titration. The stability constants ($\beta = [M_xL_y^{xn+}]/[M^{n+}]^x[L]^y$) were determined by UV−vis spectrophotometric titration at 25 °C. The experiments were carried out on a Shimuzu in a 1.0 cm quartz cell. The concentration of ligand **1** in methanol was 2.0×10^{-5} M. 0.01 M tetraethylammonium nitrate (Et_4NNO_3) was added to control the ionic strength. Each 20 μL of 0.001 M metal nitrates in methanol were titrated into 5 mL of ligand solution. After mixing vigorously for 5 min, the solution was measured in a 1.0 cm quartz cell. Such contact time was sufficient to attain the complexation equilibrium in our experiments. The obtained spectral data were treated and fitted with the HypSpec program.[45,46]

Theoretical Methods. All the theoretical calculations were carried out by using the density functional theory (DFT) method with the *Gaussian 09* package.[47] The functional used is B3LYP, which combines Becke's three-parameter functional (B3)[48] with the Lee−Yang−Parr (LYP) correlation functional.[49] For Am, Eu, Th, and U, relativistic effects were taken into consideration with the quasi-relativistic effective core potentials (RECPs).[50,51] The adopted small-core RECPs replace 60 core electrons for Am, Th, U, and 28 electrons for Eu. With regard to light atoms like C, H, O, and N, the standard Pople-style polarized valence triple-ξ 6-311G(d,p) basis set was used for geometry optimization.

All the complexes were optimized at the B3LYP/6-311G(d,p)/RECP level of theory in the gas phase. Harmonic vibrational frequencies were calculated to verify the minimum character of the optimized structures. The natural atomic charges and Wiberg bond indices (WBIs) were calculated by natural bond orbital (NBO) analyses at the same method. The frequencies of all the chemical species were calculated at the same level of theory on the basis of the optimized geometries. Other detailed methods were the same as our previous studies.[14,28,32,52,53] Theoretical Cartesian coordinates of the optimized structures are listed in Table S5, SI.

dx.doi.org/10.1021/ic402784c | *Inorg. Chem.* XXXX, XXX, XXX−XXX

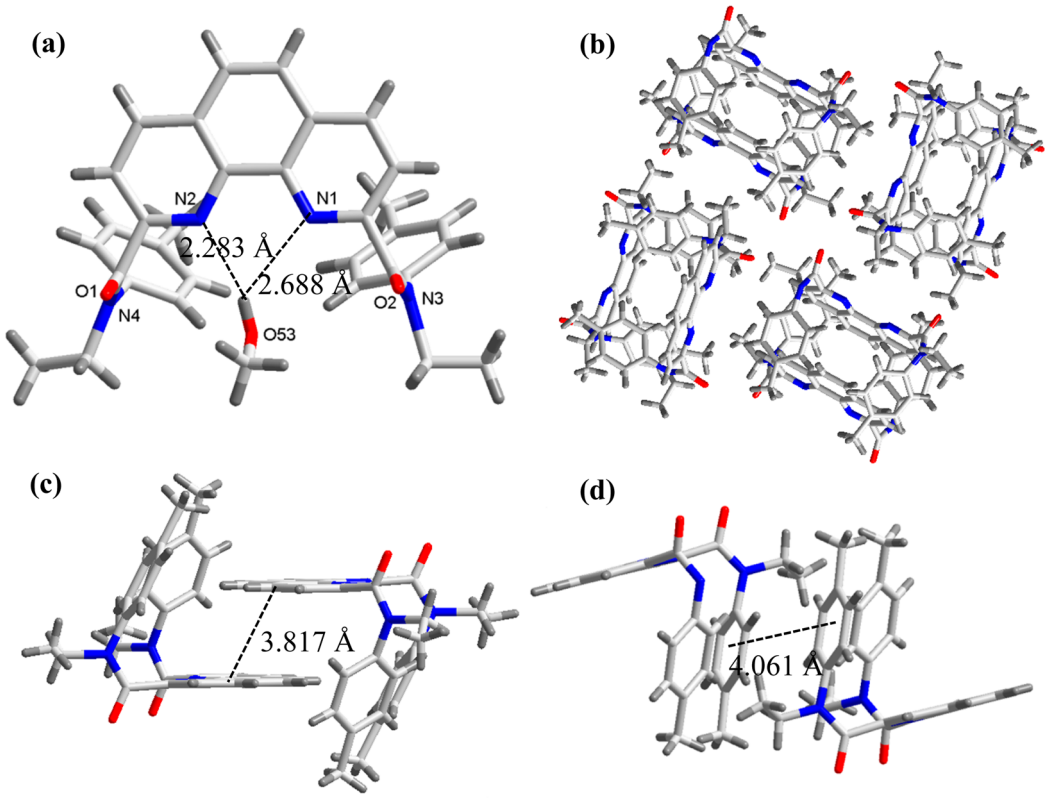

Figure 2. X-ray crystal structure of ligand **1**, (a) single molecule; (b) packing pattern; (c) $\pi-\pi$ stacking between phenanthroline and phenanthroline; (d) $\pi-\pi$ stacking between phenyl and phenyl. The anions and solvents have been omitted for clarity.

RESULTS AND DISCUSSION

Syntheses and Ligand Structure. As we know, extractants containing amide groups have strong affinity for light actinides in high oxidation states.[32,34,36,37] Additionally, phenanthroline-based ligands were reported to have high selectivity for MA(III) over Ln(III).[16,24,27,31,54] Thus, we intended to design a novel ligand for separating all actinides from other fission products by combining amide groups with the phenanthroline skeleton.

N,*N*′-Diethyl-*N*,*N*′-ditolyl-2,9-diamide-1,10-phenanthroline (Et-Tol-DAPhen, **1**) was synthesized in four steps using 2,9-dimethyl-1,10-phenanthroline as the starting material (Scheme 1). The first two steps with high yields (>80%) were carried out according to the reported literatures.[41,42] To avoid the reaction of the diacyl chloride product with water during storage, we developed a one-pot method to synthesize the ligand **1**. After the diacid product was reacted with thionyl chloride and the excess solvent was removed, dichloromethane and *N*-ethyl-*p*-toluidine were added in the same flask. Additionally, an organic base, triethylamine, was introduced to accelerate the reaction. The ligand **1** could be readily synthesized on a multigram scale in reasonable yields.

Slow evaporation of the solution of ligand **1** in methanol over three days afforded colorless crystals suitable for X-ray analysis. The crystal structure of ligand **1** and its packing patterns are shown in Figure 2. The ligand structure (Figure 2a) has a near C_2 symmetry, with two tolyl groups on one side and two oxygen atoms on the opposite side. The torsion angles of C17−N3−C22−C9 and C16−N4−C13−C7 are −4.188° and −4.679°, respectively. One methanol molecule is located in the cavity of ligand **1** with hydrogen bonding. The H---N1 and H---N2 bond lengths are 2.283 and 2.688 Å, respectively. The ligand crystals are formed with multiple $\pi-\pi$ stackings, which construct quantities of nanosized channels (Figure 2b). The $\pi-\pi$ stacking distances between two neighboring phenanthroline moieties (Figure 2c) are 3.817 Å, while those between two neighboring tolyl moieties are 4.061 Å (Figure 2d).

Solvent Extraction Studies. The effect of HNO_3 concentration on the extraction properties of Th(IV), U(VI), Am(III), and Eu(III) by ligand **1** was investigated in cyclohexanone solvent. As shown in Figure 3a, the Et-Tol-DAPhen ligand exhibits extremely high extraction ability toward all actinides even in absence of any synergists. The distribution ratios of Th(IV), U(VI), and Am(III) are determined to be 205, 25, and 6 in 1.0 M HNO_3, respectively. Additionally, it is obvious that the distribution ratios of all actinides are higher than that of Eu(III) across the range of HNO_3 concentrations. The separation factors (*SF*) of Th(IV), U(VI), and Am(III) toward Eu(III) are 2277, 277, and 67 in 1.0 M HNO_3, respectively. Considering Pu(IV) possesses the same oxidation states and similar chemical properties with Th(IV), the Et-Tol-DAPhen ligand should have reasonable extractability toward Pu(IV). To the best of our knowledge, with respect to the group separation of actinides using a single extractant, the distribution ratios and selectivity for all actinides over lanthanides that we achieved in highly acidic solution in this case are the most competitive compared to the previous work.[38,39] Generally, extractants containing soft sulfur or nitrogen atoms are preferred to recognize minor actinides (Am, *Cm*) over lanthanides, whereas ligands containing hard oxygen atoms favor light actinides (U, Th, Np, Pu). If one wants to separate all actinides from lanthanides in acidic solution, two extractants containing soft and hard atoms, respectively, should be combined in one solvent.[5−10] In this

dx.doi.org/10.1021/ic402784c | *Inorg. Chem.* XXXX, XXX, XXX−XXX

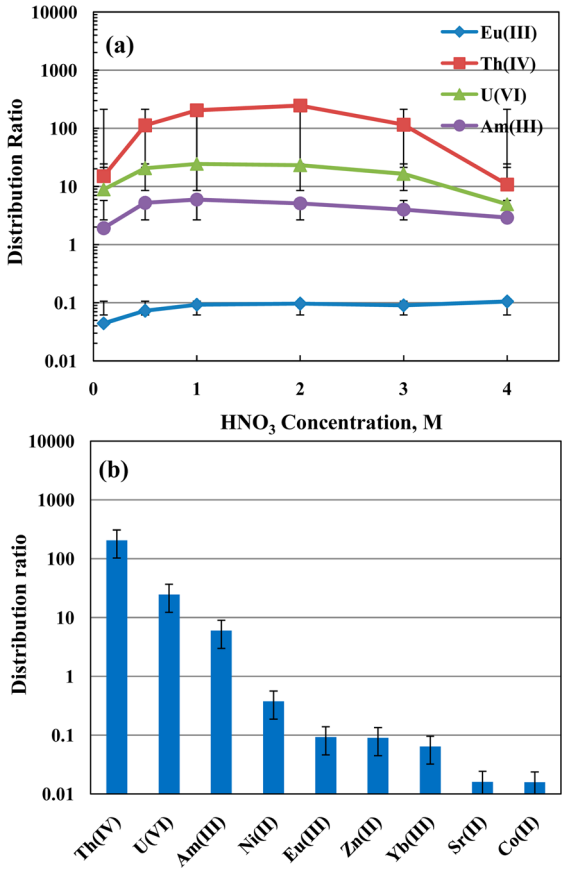

Figure 3. (a) Extraction properties of some actinides and lanthanides by Et-Tol-DAPhen as a function of HNO_3 concentration in cyclohexanone. (b) Comparison of extraction ability of different metal ions by Et-Tol-DAPhen in 1.0 M HNO_3 solution.

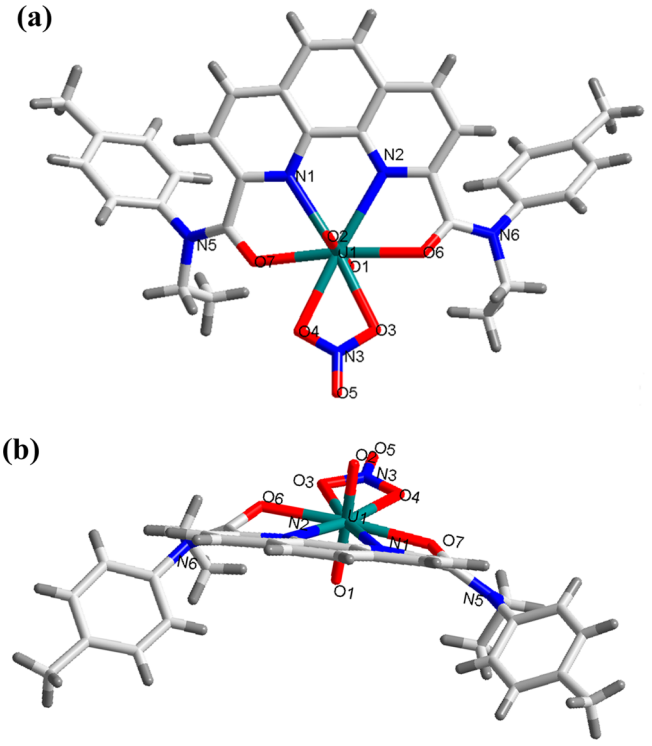

Figure 4. X-ray crystal structure of the $[UO_2(\mathbf{1})NO_3]^+$ **2**. (a) View in front. (b) View from the top. The anion and solvent molecules have been omitted for clarity. Selected bond lengths (Å): U1−O1 1.737(9), U1−O2 1.750(9), U1−O7 2.399(8), U1−O6 2.411(9), U1−O4 2.512(9), U1−O3 2.527(10), U1−N1 2.587(10), U1−N2 2.604(9). Blue green, blue, red, gray, and dark gray colors denote U, N, O, C, and H atoms, respectively.

work, we combined soft nitrogen atoms and hard oxygen atoms in one ligand and achieved high extraction ability and excellent selectivity for all actinides. Besides, the Et-Tol-DAPhen ligand shows weak extraction ability for the fission and corrosion products, such as Yb(III), Sr(II), Co(II), Ni(II), and Zn(II) (Figure 3b). Thus, the Et-Tol-DAPhen ligand is quite promising in the group separation of actinides from nuclear wastes.

UO_2^{2+} and Th^{4+} Complexes Structures. To provide structural information for investigating the complexation behaviors and extraction mechanisms, we synthesized the complex crystals of ligand **1** with uranium(VI) and thorium(IV).

Yellow crystals **2** suitable for X-ray measurements were obtained by slow evaporation of the solution of $UO_2(NO_3)_2 \cdot 6H_2O$ and ligand **1** in acetone/water (vol/vol, 1:1). As displayed in Figure 4, each ligand is bound to one UO_2^{2+} through two nitrogen atoms of the phenanthroline moiety together with two oxygen atoms of the amide moieties. The average bond distance of U−N is 2.596 Å, which is slightly longer than that of unsubstituted phenanthroline dicarboxylic acid complexes (2.557 Å).[55] In the Cambridge Structural Database (CSD),[56,57] eight structures of uranyl 1,10-phenanthroline complexes (Figure S1, SI) can be found. Normally, the U−N bond distances are in the range of 2.557−2.652 Å. A comparison of the bond lengths between U(VI) and nitrogen atoms indicates that the structure feature of **1** is similar to the uranyl 1,10-phenanthroline complexes in the database. The average distance between U(VI) and oxygen atoms of the amide moieties in **1** is 2.406 Å, whereas the U−O bond distance of 2.351 Å is found in the unsubstituted phenanthroline dicarboxylic acid.[55] Such difference might be due to the decrease of affinity for UO_2^{2+} after the introduction of ethyl and tolyl groups into the amide moieties of **1**. Additionally, the uranium atom is bound to one nitrate anion with U−O bond distance of 2.519 Å. Another nitrate anion is in the second coordination layer for keeping the charge balance. The uranyl is almost located in the plane of phenanthroline with an O6−U1−O7 angle of 171.593°. Two tolyl groups are still in the same side similar to ligand **1** (Figure 2). Low distortion of the ligand structure after complexing with uranyl ion indicates that the preorganized ligand **1** is suitable for adopting metal ions with large ionic radii such as UO_2^{2+}. That might be the reason that ligand **1** shows such high extraction ability for UO_2^{2+}.

$Th(\mathbf{1})(NO_3)_4$ complexes **3** suitable for X-ray measurements were prepared using the same method as for the uranyl complex. The structure of $Th(\mathbf{1})(NO_3)_4$ is shown in Figure 5. The Et-Tol-DAPhen ligand is bound to Th^{4+} through two nitrogen atoms of the phenanthroline moiety along with two oxygen atoms of the amide moieties. Interestingly, the 1:1 structure of thorium complex with ligand **1** is quite different from the 1:2 structure of the unsubstituted phenanthroline dicarboxylic acid.[55] The steric effect of the substituent groups and the strong coordinating ability of nitrate ions is the probable reason for 1:1 coordination of ligand **1** with Th^{4+}. The average Th−N bond distance is 2.692 Å. In the CSD database,[56,57] we found three structures of thorium 1,10-

dx.doi.org/10.1021/ic402784c | Inorg. Chem. XXXX, XXX, XXX−XXX

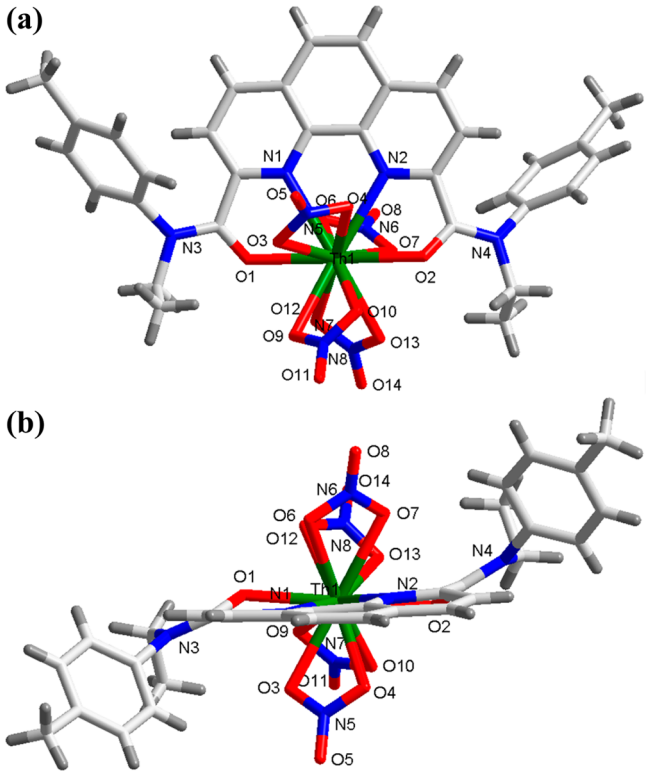

Figure 5. X-ray crystal structure of the Th(**1**)$(NO_3)_4$ complex **3**. (a) View in front. (b) View from top. The solvent molecules have been omitted for clarity. Selected bond lengths (Å): Th−O1 2.447(4), Th−O2 2.464(5), Th−O10 2.558(5), Th−O4 2.569(5), Th−O12 2.576(5), Th−O9 2.576(5), Th−O3 2.587(5), Th−O13 2.587(5), Th−O7 2.622(5), Th−O6 2.634(5), Th−N2 2.686(5), Th−N1 2.698(5). Green, blue, red, gray, and dark gray colors denote Th, N, O, C, and H atoms, respectively.

phenanthroline complexes and only two crystal structures are available (Figure S2, SI). The Th−N bond distance of the Th(**1**)$(NO_3)_4$ complex is longer than its hydroxymethyl analogue (2.630 Å)[58] and quite similar to that of the corresponding dicarboxylic acid complex (2.693 Å).[55] Compared to hydroxymethyl analogue, the electron-withdrawing effect of C═O groups is more obvious in Et-Tol-DAPhen, decreasing the coordination ability of nitrogen atoms toward Th^{4+}. The average bond distance of Th−O_{amide} is 2.456 Å, which is a little longer than that of phenanthroline dicarboxylic acid (2.430 Å) and shorter than that of phenanthroline dihydroxymethyl (2.471 Å). This inicates that the complexation ability of Th^{4+} with oxygen atoms of different functional groups decreases in the order of carboxylic acid > amide > hydroxymethyl. Besides, thorium ion is coordinated to four nitrates anions with two locating above the phenanthroline plane and the others below the plane to achieve a coordination number of 12 for thorium. The average bond distance between thorium and oxygen atoms of nitrate anions is 2.589 Å. Compared to the $[UO_2(\mathbf{1})NO_3]^+$ structure, the orientation of tolyl groups is changed. The two tolyl groups are located in the phenanthroline plane on opposite sides (Figure 4b). The coordination of four nitrate ions to Th^{4+} makes the space too crowded to accommodate two tolyl groups at the same side. This conformation gives the complex the lowest energy to stabilize in the solid. Furthermore, the Th^{4+} is perfectly located in the phenanthroline plane with a O1−Th1−O2 angle of 179.026°, which is attributed to the preorganized structure of Et-Tol-DAPhen. The cavity of Et-Tol-DAPhen perfectly matches the size of Th^{4+}.

Stability Constant Determination. The complexation behaviors of ligand **1** with UO_2^{2+}, Th^{4+}, and Eu^{3+} were investigated in methanol by UV−vis spectrometry. The spectrophotometric titrations of ligand **1** with UO_2^{2+}, Th^{4+}, and Eu^{3+} are shown in Figure 6. All of the spectra have similar changing trends. With increasing the amounts of metal ions added, the peak of ligand **1** (273 nm) gradually decreases, and a new peak (>300 nm) denoting a metal−ligand complex appears. For every titration curve, obvious isosbestic points can be seen, which indicates that only one single complexation

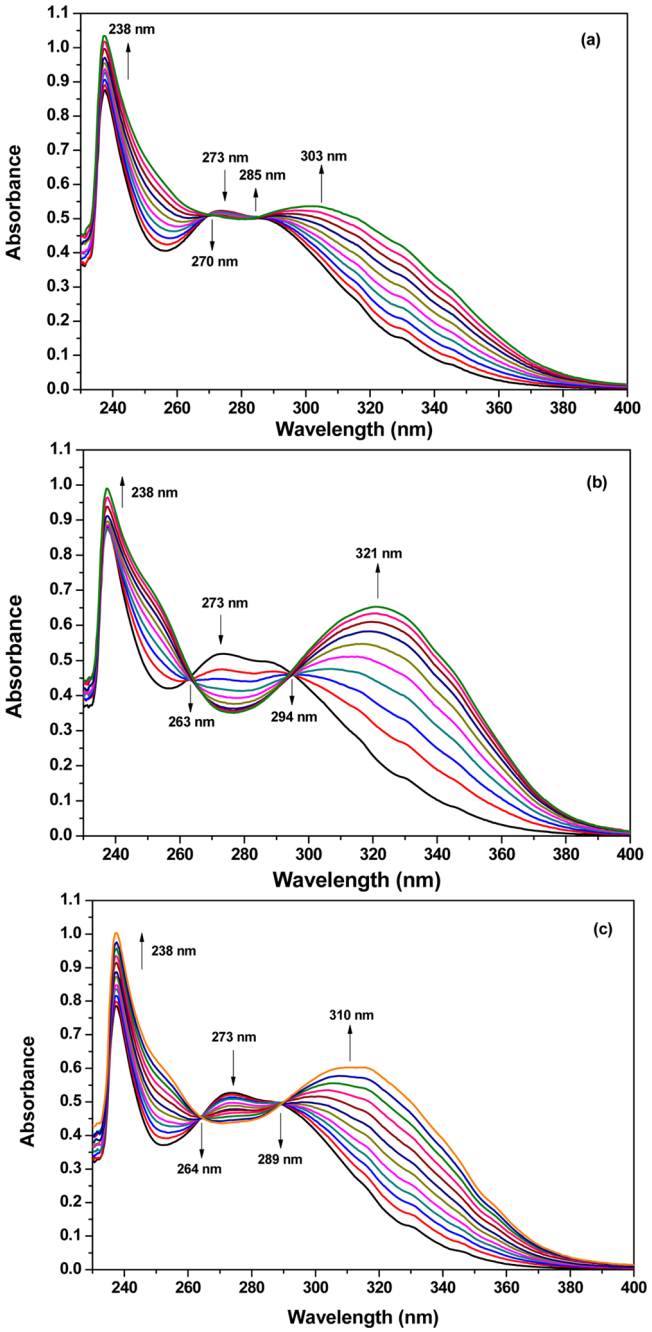

Figure 6. Spectrophotometric titration of ligand **1** (C_L = 2.0 × 10^{-5} M) with (a) $UO_2(NO_3)_2$, (b) $Th(NO_3)_4$, and (c) $Eu(NO_3)_3$ in methanol (C_M = 0−3.0 × 10^{-5} M), T = 25 °C, I = 0.01 M Et_4NNO_3.

dx.doi.org/10.1021/ic402784c | Inorg. Chem. XXXX, XXX, XXX−XXX

reaction is present. One to one stoichiometries of metal ions complexes with ligand **1** are well fitted to the experimental data by the HypSpec program.[45,46] The 1:1 complexes of UO_2^{2+} and Th^{4+} are consistent with those found in the solid state.

The calculated stability constants (log β) are listed in Table 1. The corresponding stability constants of 1,10-phenanthroline-2,9-dicarboxamide (PDAM)[60,61] and 1,10-phenanthroline-2,9-dicarboxylic acid (PDA)[55,62] are also given for comparison. The results show that ligand **1** has reasonable complexation ability for actinides and lanthanides with log $\beta \approx 4$. The stability constants of UO_2^{2+} and Th^{4+} are somewhat higher than that of Eu^{3+}, which agree well with the higher distribution coefficients for actinides in the solvent extraction experiments. With different solution and metal salts, the stability constants of ligand **1** and PDAM for actinides and lanthanides hold almost the same order of magnitude. This suggested that the coordination mode and capability of 1,10-phenanthroline-2,9-dicarboxamide with metal ions did not change much after further functionalization. However, its dicarboxylic acid analogue has extremely high stability constants for actinides and lanthanides. Obviously, the complexation ability of the carboxylic acid with metal ions is stronger than that of amide.

Table 1. Stability Constants (log β) for Some Actinide and Lanthanide Complexes with Ligand 1, PDAM, and PDA in Methanol Determined by UV−Vis Spectrometry

metal ion	ionic radius (Å)	complexation reaction	log β^b	log β_1^c	log β_2^d
UO_2^{2+}	0.95[a]	$UO_2^{2+} + L = UO_2L^{2+}$	4.68	4.33	>13
Th^{4+}	0.94	$Th^{4+} + L = ThL^{4+}$	4.39	5.01	25.7
Eu^{3+}	0.89	$Eu^{3+} + L = EuL^{3+}$	3.81	4.17	–

[a]This is the apparent size because of no ionic radius for irregular-shaped UO_2^{2+}.[59] [b]Ligand **1** (2.0×10^{-5} M) in methanol, metal nitrates, T = 25 °C, I = 0.01 M Et_4NNO_3. [c]1,10-Phenanthroline-2,9-dicarboxamide (PDAM, 2.0×10^{-5} M) in deionized water, metal perchlorates, T = 25 °C, I = 0.1 M $NaClO_4$.[60,61] [d]1,10-Phenanthroline-2,9-dicarboxylic acid (PDA, 2.0×10^{-5} M) in deionized water, metal perchlorates, T = 25 °C, I = 0.01 M $NaClO_4$.[55,62]

DFT Calculations. *Geometries and Electronic Properties of Ligand 1.* As shown in Figure 7, ligand **1** has four conformers according to the position of tolyl and ethyl groups. The relative electronic energies are 0.00, 1.95, 2.52, and 2.53 kcal/mol, respectively. The configuration (conformer 1, outward−inward) with one outward tolyl and another inward tolyl group has the lowest energy. If any tolyl group changes its position, the energy will increase. The stability of the confomers decreases in the order of outward−inward (**4**) < outward−downward (**3**) < downward−downward (**2**) < outward−outward (**1**). However, there are tiny energy differences between these four conformers. Thus, ligand **1** may form any configuration from conformers **1**−**4**, and which one exists in the solid state depends mainly on the packing effects and solvent effects.[63] Actually, we obtained the single-crystal structure of conformer **4** (Figure 2) from slow evaporation of a solution of ligand **1** in CH_3OH/CH_2Cl_2. Additionally, the configurations of ligand **1** in $UO_2(\mathbf{1})(NO_3)$ (Figure 4) and in $Th(\mathbf{1})(NO_3)_4$ (Figure 5) belong to conformer **4** and conformer **1**, respectively. Due to the steric effect of ethyl groups in the cavity, conformers **2** and **3** may not be suitable for forming complexes with other metal ions or coordinating species.

Geometries and NBO Analysis of the Complexes. To understand the coordination modes and bonding nature of

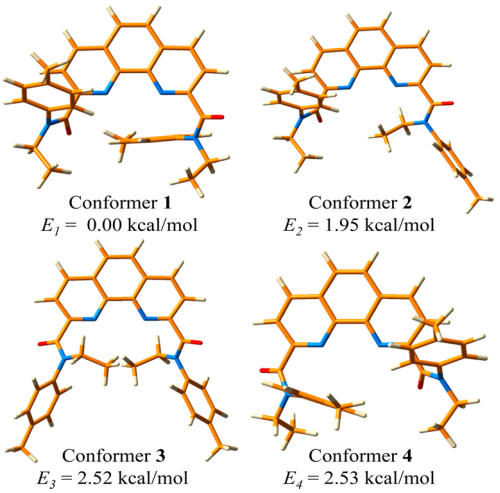

Figure 7. Optimized structures and relative electronic energies of ligand **1** in different conformers by the B3LYP method in the gas phase. Sky blue, red, orange, and white colors denote N, O, C, and H atoms, respectively.

ligand **1** with lanthanides and actinides, we optimized the structures of $Am(\mathbf{1})(NO_3)_3$, $Eu(\mathbf{1})(NO_3)_3$, $[UO_2(\mathbf{1})(NO_3)]^+$, and $Th(\mathbf{1})(NO_3)_4$ (Figure 8) at the B3LYP/6-311G(d,p)/

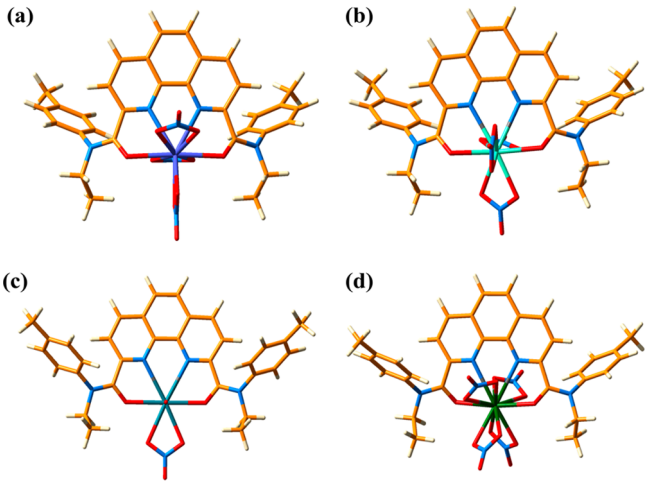

Figure 8. Optimized structures of (a) $Am(\mathbf{1})(NO_3)_3$, (b) $Eu(\mathbf{1})(NO_3)_3$, (c) $[UO_2(\mathbf{1})(NO_3)]^+$, (d) $Th(\mathbf{1})(NO_3)_4$ by the B3LYP method in the gas phase. Purple, cyan, sea green, green, sky blue, red, orange, and white colors denote Am, Eu, U, Th, N, O, C, and H atoms, respectively.

RECP level of theory in the gas phase. It is a pity that no crystals of lanthanides complexes with ligand **1** are obtained even if many endeavors have been made. Fortunately, quantum chemical calculations can help us to further understand the structures of these complexes. Similarly to most tetradentate ligands,[30,31,64] ligand **1** is bound to one metal ion through two nitrogen atoms of the phenanthroline moiety and two oxygen atoms of the amide moieties forming 1:1 complexes. For the Am^{3+} (Figure 8a) and Eu^{3+} (Figure 8b) complexes, the coordination number of metal ions is 10 with the nitrate anions in a bidentate mode. As listed in Table 2, the average bond distance of Am−N (2.678 Å) is shorter than that of Eu−N (2.729 Å). This shows that there may be more covalent characters in the Am−N bond. The bond distance of Eu−O_A

dx.doi.org/10.1021/ic402784c | Inorg. Chem. XXXX, XXX, XXX−XXX

Table 2. Calculated Bond Distances (Å), Natural Charges, and Wiberg Bond Indices (WBIs) of $Am(1)(NO_3)_3$, $Eu(1)(NO_3)_3$, $UO_2(1)(NO_3)$, and $Th(1)(NO_3)_4$ Complexes

complex	M−N	$M-O_A$	$M-O_N$	$M-N_{WBI}$	Q_M	Q_N	Q_O
$Am(1)(NO_3)_3$	2.678	2.569	2.547	0.214	1.390	−0.446	−0.597
$Eu(1)(NO_3)_3$	2.729	2.510	2.503	0.205	1.298	−0.419	−0.602
$[UO_2(1)(NO_3)]^+$	2.718	2.435	2.468	0.332	1.436	−0.419	−0.563
$Th(1)(NO_3)_4$	2.803	2.508	2.593	0.289	1.081	−0.413	−0.580

(the oxygen atom in the amides) is shorter than that of $Am-O_A$, which is indicative of stronger coordination of the oxygen atoms to Eu^{3+}. Thus, the selectivity of ligand **1** toward Am^{3+} over Eu^{3+} in the solvent extraction system may be attributed to the nitrogen atoms in the phenanthroline rather than the oxygen atom in the amides. The optimized structures of $[UO_2(1)(NO_3)]^+$ (Figure 8c) and $Th(1)(NO_3)_4$ (Figure 8d) in the gas phase are similar to the crystal structures in the solid state. It is noteworthy that the bond distances of M−N and M−O in the gas phase are longer than those of solid structures. This phenomenon is very common in theoretical calculations.[14,25,28,32,52,65] For example, the bond distances of U−N optimized by DFT method are overestimated by 0.03−0.12 Å compared to the crystal complex of 2,6-bis(5,6-dimethyl-1,2,4-triazin-3-yl)pyridine (Me-BTP) with uranyl ion.[65] These differences may originate from the neglect of electron correlation as well as crystal packing effects and solvent effects in the optimization.

To explore the bonding nature of the M−N bonds, the natural bonding orbital (NBO) analyses of all the 1:1 species were performed at the B3LYP/6-311G(d,p)/RECP level of theory. The Wiberg bond index (WBI) in NBO analysis is widely accepted to measure the degree of covalency.[32,53] As shown in Table 2, the WBIs of M−N bonds are in the range of 0.205−0.332. Such small values show that the interactions between metal ions and the ligand are mainly ionic and the electrostatic interaction dominates the M−N bonds. The WBIs of An−N bonds are larger than those of Eu−N, suggesting that more covalent characteristics exist in the An−N bonds. This finding agrees well with the results of solvent extraction. Additionally, the natural charges of An (Q_{An}) are also larger than those on Eu except Th, which indicates that ligand **1** has a stronger coordinating ability to An than Eu. The natural charges on the nitrogen atoms of phenanthroline (Q_N) and the oxygen atoms of amides (Q_O) are in the range of −0.446 to −0.413 and −0.602 to −0.563, respectively.

CONCLUSIONS

We have first synthesized a novel tetradentate phenanthroline-amide ligand with combined hard−soft donors. It is found that the Et-Tol-DAPhen ligand shows selective extraction ability of actinides over lanthanides from highly acidic solution. The 1:1 coordination modes are determined by X-ray crystallography for the crystal structures of Et-Tol-DAPhen with Th^{4+} and UO_2^{2+}. The stability constants of Et-Tol-DAPhen for actinides are higher than those of lanthanides, which agrees well with the higher distribution coefficients for actinides in the solvent extraction experiments. Furthermore, the results of quantum chemical calculation provide a hint that more covalency of the An−N bonds than that of Eu−N may dominate the selectivity of Et-Tol-DAPhen toward actinides. This ligand is the first efficient ligand for group separation of actinides from fission products in highly acidic solution until now, which holds promising applications in the partitioning of nuclear waste.

ASSOCIATED CONTENT

Supporting Information

X-ray crystallographic data and selected bond distances/angles of ligand **1**, UO_2^{2+} complex **2**, and Th^{4+} complex **3**, Cartesian coordinates of optimized structures. This material is available free of charge via the Internet at http://pubs.acs.org. Structures of uranyl/thorium 1,10-phenanthroline complexes in CSD database.

AUTHOR INFORMATION

Corresponding Authors

*E-mail: shiwq@ihep.ac.cn

*E-mail: zfchai@suda.edu.cn

Notes

The authors declare no competing financial interest.

ACKNOWLEDGMENTS

This work was supported by the Major Research Plan "Breeding and Transmutation of Nuclear Fuel in Advanced Nuclear Fission Energy System" of the Natural Science Foundation of China (Grant Nos. 91326202 and 91126006) and the National Natural Science Foundation of China (Grant Nos. 21201166, 11275219, 11105162, and 21261140335), the "Strategic Priority Research Program" of the Chinese Academy of Sciences (Grant No. XDA030104), and the China Postdoctoral Science Foundation (Grant No. 2013M530734).

REFERENCES

(1) Wang, S. A.; Alekseev, E. V.; Depmeier, W.; Albrecht-Schmitt, T. E. *Chem. Commun.* **2011**, *47*, 10874−10885.

(2) Salvatores, M.; Palmiotti, G. *Prog. Part. Nucl. Phys.* **2011**, *66*, 144−166.

(3) Inoue, T.; Sakata, M.; Miyashiro, H.; Matsumura, T.; Sasahara, A.; Yoshiki, N. *Nucl. Technol.* **1991**, *93*, 206−220.

(4) Blomeke, J. O.; Croff, A. G. *Nucl. Technol.* **1982**, *56*, 361−371.

(5) Whittaker, D. M.; Griffiths, T. L.; Helliwell, M.; Swinburne, A. N.; Natrajan, L. S.; Lewis, F. W.; Harwood, L. M.; Parry, S. A.; Sharrad, C. A. *Inorg. Chem.* **2013**, *52*, 3429−3444.

(6) Bell, K.; Carpentier, C.; Carrott, M.; Geist, A.; Gregson, C.; Heres, X.; Magnusson, D.; Malmbeck, R.; McLachlan, F.; Modolo, G.; Mullich, U.; Sypula, M.; Taylor, R.; Wilden, A. *Procedia Chem.* **2012**, *7*, 392−397.

(7) Aneheim, E.; Ekberg, C.; Foreman, M. R. S.; Lofstrom-Engdahl, E.; Mabile, N. *Sep. Sci. Technol.* **2012**, *47*, 663−669.

(8) Aneheim, E.; Ekberg, C.; Fermvik, A.; Foreman, M. R. S. J.; Gruner, B.; Hajkova, Z.; Kvicalova, M. *Solvent Extr. Ion. Exch.* **2011**, *29*, 157−175.

(9) Aneheim, E.; Ekberg, C.; Fermvik, A.; Foreman, M. R. S.; Retegan, T.; Skarnemark, G. *Solvent Extr. Ion. Exch.* **2010**, *28*, 437−458.

(10) Aneheim, E.; Ekberg, C.; Fermvik, A.; Foreman, M. R. S. *Nucl. Energy Environ.* **2010**, *1046*, 119−130.

(11) Hudson, M. J.; Harwood, L. M.; Laventine, D. M.; Lewis, F. W. *Inorg. Chem.* **2013**, *52*, 3414−3428.

(12) Poinssot, C.; Rostaing, C.; Baron, P.; Warin, D.; Boullis, B. *Procedia Chem.* **2012**, *7*, 358−366.

(13) Modolo, G.; Wilden, A.; Geist, A.; Magnusson, D.; Malmbeck, R. *Radiochim. Acta* **2012**, *100*, 715−725.
(14) Lan, J. H.; Shi, W. Q.; Yuan, L. Y.; Li, J.; Zhao, Y. L.; Chai, Z. F. *Coord. Chem. Rev.* **2012**, *256*, 1406−1417.
(15) Yang, Y. Q.; Luo, S. Z.; Yang, T. Z.; Hao, F. H. *Prog. Chem.* **2011**, *23*, 1345−1354.
(16) Lewis, F. W.; Hudson, M. J.; Harwood, L. M. *Synlett* **2011**, 2609−2632.
(17) Ansari, S. A.; Pathak, P.; Mohapatra, P. K.; Manchanda, V. K. *Sep. Purif. Rev.* **2011**, *40*, 43−76.
(18) Kolarik, Z. *Chem. Rev.* **2008**, *108*, 4208−4252.
(19) Banik, N. L.; Denecke, M. A.; Geist, A.; Modolo, G.; Panak, P. J.; Rothe, J. *Inorg. Chem. Commun.* **2013**, *29*, 172−174.
(20) Geist, A.; Mullich, U.; Magnusson, D.; Kaden, P.; Modolo, G.; Wilden, A.; Zevaco, T. *Solvent Extr. Ion. Exch.* **2012**, *30*, 433−444.
(21) Trumm, S.; Geist, A.; Panak, P. J.; Fanghanel, T. *Solvent Extr. Ion. Exch.* **2011**, *29*, 213−229.
(22) Kolarik, Z.; Mullich, U.; Gassner, F. *Solvent Extr. Ion. Exch.* **1999**, *17*, 23−32.
(23) Kolarik, Z.; Mullich, U.; Gassner, F. *Solvent Extr. Ion. Exch.* **1999**, *17*, 1155−1170.
(24) Lewis, F. W.; Harwood, L. M.; Hudson, M. J.; Drew, M. G.; Hubscher-Bruder, V.; Videva, V.; Arnaud-Neu, F.; Stamberg, K.; Vyas, S. *Inorg. Chem.* **2013**, *52*, 4993−5005.
(25) Narbutt, J.; Oziminski, W. P. *Dalton Trans.* **2012**, *41*, 14416−24.
(26) Lewis, F. W.; Harwood, L. M.; Krasnov, V. P. *Eur. J. Org. Chem.* **2012**, 1509−1519.
(27) Lewis, F. W.; Harwood, L. M.; Hudson, M. J.; Drew, M. G. B.; Wilden, A.; Sypula, M.; Modolo, G.; Vu, T.-H.; Simonin, J.-P.; Vidick, G.; Bouslimani, N.; Desreux, J. F. *Procedia Chem.* **2012**, *7*, 231−238.
(28) Lan, J. H.; Shi, W. Q.; Yuan, L. Y.; Feng, Y. X.; Zhao, Y. L.; Chai, Z. F. *J. Phys. Chem. A* **2012**, *116*, 504−511.
(29) Hubscher-Bruder, V.; Haddaoui, J.; Bouhroum, S.; Arnaud-Neu, F. *Inorg. Chem.* **2010**, *49*, 1363−1371.
(30) Foreman, M. R. S.; Hudson, M. J.; Drew, M. G. B.; Hill, C.; Madic, C. *Dalton Trans.* **2006**, 1645−1653.
(31) Lewis, F. W.; Harwood, L. M.; Hudson, M. J.; Drew, M. G. B.; Desreux, J. F.; Vidick, G.; Bouslimani, N.; Modolo, G.; Wilden, A.; Sypula, M.; Vu, T. H.; Simonin, J. P. *J. Am. Chem. Soc.* **2011**, *133*, 13093−13102.
(32) Wang, C. Z.; Lan, J. H.; Zhao, Y. L.; Chai, Z. F.; Wei, Y. Z.; Shi, W. Q. *Inorg. Chem.* **2013**, *52*, 196−203.
(33) Nash, K. L.; Johnson, G.; Brigham, D.; Marie, C.; Grimes, T. S.; Braley, J. C. *Procedia Chem.* **2012**, *7*, 45−50.
(34) Ansari, S. A.; Pathak, P.; Mohapatra, P. K.; Manchanda, V. K. *Chem. Rev.* **2012**, *112*, 1751−1772.
(35) Gelis, A. V.; Vandegrift, G. F.; Bakel, A.; Bowers, D. L.; Hebden, A. S.; Pereira, C.; Regalbuto, M. *Radiochim. Acta* **2009**, *97*, 231−232.
(36) Malmbeck, R.; Courson, O.; Pagliosa, G.; Romer, K.; Satmark, B.; Glatz, J. P.; Baron, P. *Radiochim. Acta* **2000**, *88*, 865−871.
(37) Courson, O.; Lebrun, M.; Malmbeck, R.; Pagliosa, G.; Romer, K.; Satmark, B.; Glatz, J. P. *Radiochim. Acta* **2000**, *88*, 857−863.
(38) Marie, C.; Miguirditchian, M.; Guillaumont, D.; Tosseng, A.; Berthon, C.; Guilbaud, P.; Duvail, M.; Bisson, J.; Guillaneux, D.; Pipelier, M.; Dubreuil, D. *Inorg. Chem.* **2011**, *50*, 6557−6566.
(39) Marie, C.; Miguirditchian, M.; Guillaneux, D.; Bisson, J.; Pipelier, M.; Dubreuil, D. *Solvent Extr. Ion. Exch.* **2011**, *29*, 292−315.
(40) Bisson, J.; Berthon, C.; Berthon, L.; Boubals, N.; Dubreuil, D.; Charbonnel, M. C. *Procedia Chem.* **2012**, *7*, 13−19.
(41) Chandler, C. J.; Deady, L. W.; Reiss, J. A. *J. Heterocycl. Chem.* **1981**, *18*, 599−601.
(42) Chandler, C. J.; Deady, L. W.; Reiss, J. A.; Tzimos, V. *J. Heterocycl. Chem.* **1982**, *19*, 1017−1019.
(43) *SMART and SAINT* (software packages); Siemens Analytical X-ray Instruments, Inc.: Madison, WI, 1996.
(44) *SHELXTL Program*, version 5.1; Siemens Industrial Automation, Inc.: Madison, WI, 1997.
(45) Gans, P.; Sabatini, A.; Vacca, A. *Talanta* **1996**, *43*, 1739−1753.
(46) Alderighi, L.; Gans, P.; Ienco, A.; Peters, D.; Sabatini, A.; Vacca, A. *Coord. Chem. Rev.* **1999**, *184*, 311−318.
(47) Frisch, M. J.; Trucks, G. W.; Schlegel, H. B.; Scuseria, G. E.; Robb, M. A.; Cheeseman, J. R.; Scalmani, G.; Barone, V.; Mennucci, B.; Petersson, G. A.; Nakatsuji, H.; Caricato, M.; Li, X.; Hratchian, H. P.; Izmaylov, A. F.; Bloino, J.; Zheng, G.; Sonnenberg, J. L.; Hada, M.; Ehara, M.; Toyota, K.; Fukuda, R.; Hasegawa, J.; Ishida, M.; Nakajima, T.; Honda, Y.; Kitao, O.; Nakai, H.; Vreven, T.; Montgomery, J. A., Jr.; Peralta, J. E.; Ogliaro, F.; Bearpark, M.; Heyd, J. J.; Brothers, E.; Kudin, K. N.; Staroverov, V. N.; Kobayashi, R.; Normand, J.; Raghavachari, K.; Rendell, A.; Burant, J. C.; Iyengar, S. S.; Tomasi, J.; Cossi, M.; Rega, N.; Millam, J. M.; Klene, M.; Knox, J. E.; Cross, J. B.; Bakken, V.; Adamo, C.; Jaramillo, J.; Gomperts, R.; Stratmann, R. E.; Yazyev, O.; Austin, A. J.; Cammi, R.; Pomelli, C.; Ochterski, J. W.; Martin, R. L.; Morokuma, K.; Zakrzewski, V. G.; Voth, G. A.; Salvador, P.; Dannenberg, J. J.; Dapprich, S.; Daniels, A. D.; Farkas, Ö.; Foresman, J. B.; Ortiz, J. V.; Cioslowski, J.; Fox, D. J. *Gaussian 09*, Revision A.1; Gaussian, Inc.: Wallingford CT, 2009.
(48) Becke, A. D. *Phys. Rev. A* **1988**, *38*, 3098−3100.
(49) Lee, C. T.; Yang, W. T.; Parr, R. G. *Phys. Rev. B* **1988**, *37*, 785−789.
(50) Dolg, M.; Stoll, H.; Preuss, H. *J. Chem. Phys.* **1989**, *90*, 1730−1734.
(51) Kuchle, W.; Dolg, M.; Stoll, H.; Preuss, H. *J. Chem. Phys.* **1994**, *100*, 7535−7542.
(52) Lan, J. H.; Shi, W. Q.; Yuan, L. Y.; Zhao, Y. L.; Li, J.; Chai, Z. F. *Inorg. Chem.* **2011**, *50*, 9230−9237.
(53) Wang, C. Z.; Shi, W. Q.; Lan, J. H.; Zhao, Y. L.; Wei, Y. Z.; Chai, Z. F. *Inorg. Chem.* **2013**, *52*, 10904−11.
(54) Galletta, M.; Scaravaggi, S.; Macerata, E.; Famulari, A.; Mele, A.; Panzeri, W.; Sansone, F.; Casnati, A.; Mariani, M. *Dalton Trans.* **2013**, *42*, 16930−16938.
(55) Dean, N. E.; Hancock, R. D.; Cahill, C. L.; Frisch, M. *Inorg. Chem.* **2008**, *47*, 2000−2010.
(56) Bruno, I. J.; Cole, J. C.; Edgington, P. R.; Kessler, M.; Macrae, C. F.; McCabe, P.; Pearson, J.; Taylor, R. *Acta Crystallogr., Sect. B* **2002**, *58*, 389−397.
(57) Allen, F. H. *Acta Crystallogr., Sect. B* **2002**, *58*, 380−388.
(58) Gephart, R. T.; Williams, N. J.; Reibenspies, J. H.; De Sousa, A. S.; Hancock, R. D. *Inorg. Chem.* **2008**, *47*, 10342−10348.
(59) Shannon, R. D. *Acta Crystallogr., Sect. A* **1976**, *32*, 751−767.
(60) Merrill, D.; Harrington, J. M.; Lee, H. S.; Hancock, R. D. *Inorg. Chem.* **2011**, *50*, 8348−8355.
(61) Merrill, D.; Hancock, R. D. *Radiochim. Acta* **2011**, *99*, 161−166.
(62) Williams, N. J.; Dean, N. E.; VanDerveer, D. G.; Luckay, R. C.; Hancock, R. D. *Inorg. Chem.* **2009**, *48*, 7853−7863.
(63) Boubals, N.; Drew, M. G. B.; Hill, C.; Hudson, M. J.; Iveson, P. B.; Madic, C.; Russell, M. L.; Youngs, T. G. A. *J. Chem. Soc., Dalton Trans.* **2002**, 55−62.
(64) Hancock, R. D. *Chem. Soc. Rev.* **2013**, *42*, 1500−1524.
(65) Berthet, J. C.; Thuery, P.; Dognon, J. P.; Guillaneux, D.; Ephritikhine, M. *Inorg. Chem.* **2008**, *47*, 6850−6862.

dx.doi.org/10.1021/ic402784c | *Inorg. Chem.* XXXX, XXX, XXX−XXX